



## 45 1. Introduction

46 The *apolipoprotein e4* (*APOEε4*) allele is a strong genetic risk factor for Alzheimer's Disease (AD)<sup>1</sup>.  
47 Despite being widely recognised for its role in lipid transport<sup>2</sup>, amyloid beta clearance<sup>3</sup>, and  
48 neurofibrillary tangle formation<sup>4</sup>, the impact of *APOEε4* on brain function and structure might begin  
49 long before AD-related pathology occurs.

50 Functional brain imaging studies have shown altered brain function in *APOEε4* carriers already  
51 before the onset of clinical symptoms, specifically in the activity and connectivity of resting-state  
52 networks in middle-aged individuals (reviewed<sup>5,6</sup>). A decrease in functional connectivity in the  
53 areas of the Default Mode Network (DMN) has been consistently reported in middle-aged adults.  
54 The findings in young adults are much more mixed with studies reporting both an increase<sup>7-9</sup> and a  
55 decrease<sup>9-13</sup>. Only the medial visual network<sup>13</sup> showed alterations in young *APOEε4* carriers  
56 beyond the findings from the DMN. There were no differences in other resting-state networks  
57 including the executive/frontoparietal, visual, sensorimotor<sup>10,13</sup>, dorsoattentional, salience, and  
58 language<sup>10</sup> and auditory networks<sup>13</sup>.

59 The inconsistencies in findings might be partly explained by the ethnicity of the participants<sup>14</sup>.  
60 While ethnicity is not consistently reported across all the studies, studies that were conducted on  
61 the Chinese Han population showed similarities in the directionality of connectivity differences. The  
62 connectivity decreased in the angular gyrus<sup>10</sup>, dorsolateral prefrontal cortex<sup>12</sup>, and between the  
63 hippocampus and praecuneus/posterior cingulate cortex and subgenual anterior cingulate cortex<sup>9</sup>.  
64 Moreover, recent follow-up research shows that the whole-brain connectivity in the young Chinese  
65 Han population decreases over time<sup>15</sup>. Additionally, evidence from other neuroimaging studies  
66 suggests that the presence of the *APOEε4* allele modulates brain structure and function in this  
67 population in young adulthood beyond connectivity<sup>16,17</sup>.

68 Further, the inconsistencies in the directionality observed across young adulthood might relate to  
69 subtle differences in brain organisation of resting-state networks in early adulthood. Therefore,  
70 using the measures that are more sensitive to subtle nuances and offer a more holistic view of  
71 brain alterations might offer deeper insights. Graph theoretical analysis has become an important  
72 tool in the examination of brain organisation and reorganisation at various stages of neurological  
73 and psychiatric disorders<sup>18</sup>. This approach enables a more comprehensive understanding of the  
74 intricate relationship of dynamic changes within the neural circuits associated with different stages  
75 of neurological and psychiatric conditions.

76 In neurodegeneration, studies suggest that graph properties undergo progressive alterations in  
77 Mild Cognitive Impairment (MCI) and AD<sup>19</sup>. These alterations are also evident in the functional  
78 networks of *APOEε4* carriers experiencing subjective cognitive decline<sup>20</sup>. Moreover, by using the  
79 combination of graph theory and machine learning approaches, Hojjati and colleagues<sup>21</sup> identified  
80 areas underlying conversion from MCI to AD.

81 While some evidence exists from the cognitively healthy older population at risk of AD<sup>22</sup>, further  
82 exploration in pre-symptomatic stages remains limited with a notable gap in the literature  
83 concerning graph theoretical studies of functional networks in young adults (reviewed<sup>23</sup>). It is  
84 unclear what exact connectivity differences occur in at-risk populations and how early they begin.  
85 The lack of evidence emphasises the necessity for systematic exploration in this critical  
86 demographic. Investigating early disease vulnerabilities and monitoring disease progression across  
87 the lifespan is critical to understanding the nature of the disorder fully and to developing potential  
88 therapeutic and preventative interventions that might include risk factor modification.

89 In this work, we used a graph theoretical approach to investigate the behaviour of the resting-state  
90 networks in young *APOEε4* carriers. We analysed seven networks of interest: the DMN,  
91 sensorimotor, visual, salience, dorsoattentional, language, and frontoparietal networks. By  
92 exploring these networks, we aimed to unveil the pattern of connectivity alterations associated with  
93 genetic vulnerability in the brain. We were interested in the properties that relate to network  
94 communication, information flow, and organisation; namely, Betweenness Centrality, Closeness  
95 Centrality, Degree Centrality, Average Path Length, Global Efficiency, and Clustering Coefficient.

## 96 2. Methods

### 97 2.1. Study sample

98 A total of 392 young cognitively healthy self-declared Chinese Han college students from  
99 Southwest University participated in this study as an extension of the PREVENT-Dementia study<sup>24</sup>.  
100 The study followed the regulations of the PREVENT-Dementia and Southwest University.  
101 Research ethics was provided by Southwest University's local ethics committee. All participants  
102 provided informed written consent.

103 All participants provided a saliva sample for DNA genotyping, which was determined by the Mass  
104 Array system (Agena iPLEX assay, San Diego, USA). For the purpose of this study, the  
105 participants were classified as either carriers (i.e., at least one copy of the *APOEε4* allele) or non-  
106 carriers (i.e., no copy of the *APOEε4* allele). A subset of 155 participants underwent neuroimaging  
107 using MRI. After excluding data from participants with poor segmentation or acquisition quality, a  
108 final dataset resulted in 129 participants. In total, there were 27 carriers (female = 16) and 102  
109 non-carriers (female = 54). There were no significant differences between the gender of carriers  
110 (59% female) and non-carriers (53% female), age of carriers (19.6±0.98) and non-carriers  
111 (19.6±0.9), and years of education of carriers (12.9±0.55) and non-carriers (13.1±0.59).

### 112 2.2. Neuroimaging acquisition and pre-processing

113 MRI imaging data were acquired on a 3T Siemens whole-body scanner at Southwest University.  
114 Participants were instructed to keep their eyes closed and not to think about anything specific while

115 they were scanned at rest. The study protocol and pre-processing are identical to our previously  
116 published work<sup>10</sup>.

117 In brief, resting-state echo planar images and T1-weighted MPRAGE anatomical images were  
118 obtained. Neuroimaging pre-processing and functional connectivity analysis were performed using  
119 the CONN software (<https://www.nitrc.org/projects/conn>, RRID:SCR\_009550) and in-house  
120 MatLab scripts (MathWorks, Natick, MA). The pre-processing sequence in the CONN included  
121 motion estimation and correction, correction for inter-slice differences in acquisition time, outlier  
122 detection, segmentation, MNI152 co-registration, and smoothing with a Gaussian kernel of 8mm  
123 full-width half maximum. In addition, functional data were denoised by regressing potential  
124 confounding effects characterised by white matter timeseries, cerebrospinal fluid timeseries,  
125 motion parameters and their first-order derivatives, followed by bandpass frequency filtering of the  
126 BOLD timeseries between 0.008 Hz and 0.09 Hz.

127 The scans were then parcellated into resting-state networks using the Oxford-Harvard atlas<sup>25-27</sup>,  
128 which is commonly used in neuroimaging software, and hence provides a widely accepted  
129 reference for brain region parcellation. In additional analyses, the resulting networks from the  
130 Independent Component Analysis (ICA) and the templates from the Power's atlas<sup>28</sup> were used to  
131 compare the results. We were interested in seven main resting-state networks: the DMN,  
132 sensorimotor, visual, salience, dorsoattentional, frontoparietal (executive), and language networks  
133 (Fig 1).

### 134 2.3. First- and second-level analysis

135 Regions of interest connectivity matrices were estimated characterising the patterns of functional  
136 connectivity. Functional connectivity strength was represented by Fisher-transformed bivariate  
137 correlation coefficients from a weighted general linear model (GLM), defined separately for each  
138 pair of target areas, modelling the association between their BOLD signal timeseries. To  
139 compensate for possible transient magnetisation effects at the beginning of each run, individual  
140 scans were weighted by a step function convolved with an SPM canonical haemodynamic  
141 response function and rectified.

142 Group-level analyses were performed using a GLM. For each individual voxel a separate GLM was  
143 estimated, first-level connectivity measures at this connection as dependent variables, and groups  
144 as independent variables. Inferences were performed at the level of individual clusters, based on  
145 parametric statistics from Gaussian Random Field theory. Results were thresholded using a  
146 combination of  $p < 0.05$  connection level threshold, a cluster-forming  $p < 0.001$  voxel-level threshold,  
147 and a corrected  $p$ -FDR  $< 0.05$  cluster-size threshold. The data were subsequently entered into a  
148 graph theory analysis.

### 149 2.4. Graph theoretical analysis

150 Graphs are data structures that model pairwise relations between network components. When  
151 applied to fMRI data, ‘nodes’ represent different brain regions and ‘edges’ represent connections  
152 between them.

153 Subsets of regions of interest were selected for each network using available regions from the  
154 Oxford-Harvard atlas, which were then analysed in the second-level FDR-corrected within-network  
155 analyses with groups as factors (*APOEε4* carriers vs non-carriers), and age, gender, and years of  
156 education as covariates. A binary connectivity matrix is obtained by thresholding the values of the  
157 correlation matrix. This step is crucial to eliminate spurious connections in the data; however, the  
158 choice of the threshold is often arbitrary, and the different methods of thresholding may lead to  
159 substantial variability in the data<sup>29</sup>. Since we were interested in retaining the strongest connections,  
160 we utilised the cost method with the threshold of 0.15 to keep the 15% of the strongest connections.  
161 In additional analyses, we explored alternative thresholding by using the z-scores.

162 Seven graph theoretical properties were explored to assess the topological patterns of different  
163 networks, namely the measures of centrality (i.e., Betweenness Centrality, Closeness Centrality,  
164 Degree Centrality) and the measures of network structure and efficiency (i.e., Average Path Length,  
165 Global Efficiency, Clustering Coefficient). A detailed description of mathematical calculations and  
166 roles of each property can be found elsewhere<sup>30,31</sup> and is summarised in Table 1.

167 Briefly, Betweenness Centrality measures the number of the shortest paths running through a node,  
168 identifying critical hubs for efficient information flow. Closeness Centrality assesses how closely  
169 connected a node is to others, pinpointing key locations essential for efficient information transfer.  
170 Average Path Length of a network is calculated as the average number of steps along the shortest  
171 paths for all possible pairs of nodes in the network, so it reflects the typical distance between pairs  
172 of nodes in the network. Global efficiency averages the inverses of the shortest path lengths  
173 between all pairs of nodes in the network, representing effective communication across the entire  
174 network. Clustering coefficient measures which nodes in the network tend to cluster together,  
175 indicating local interconnectedness. Degree Centrality refers to the number of connections per  
176 node and thus reflects the importance of a node in the network.

Table 1. The summary of the Graph Theory properties studied in the present article.

GT Property	Calculation	Interpretation
Global Efficiency	Average of reciprocal shortest paths	Efficient information exchange across the network
Betweenness	Fraction of shortest paths	Critical nodes influencing information flow

Centrality	through a node	
Average Path Length	Average steps along shortest paths	Typical distance between nodes in the network
Clustering Coefficient	Proportion of neighbours connected to each other	Local interconnectedness; higher values indicate more cliquishness
Degree centrality	Number of edges connected to a node	Node connectivity; higher degrees may indicate more influence
Closeness Centrality	Reciprocal sum of shortest path distances	Emphasizes nodes with short distances for efficient information exchange

177

178 **3. Results**

179 **3.1. Whole-brain connectivity differences**

180 To assess the baseline whole-brain connectivity differences between *APOEε4* carriers and non-  
 181 carriers, the Oxford-Harvard atlas was used to parcellate the brain into 48 cortical and 21  
 182 subcortical regions. The graph theoretical analysis of all regions was then conducted using the  
 183 same methods as for the analysis of the networks. There were no significant differences found  
 184 between the *APOEε4* carriers and non-carriers on any of the graph theoretical measures (p-  
 185 FDR>0.05).

186 **3.2. Graph Theory differences between the *APOEε4* carriers and non-carriers**

187 Graph Theory analysis revealed differences in functional connectivity between young *APOEε4*  
 188 carriers and non-carriers in four networks in the Average Path Length and Closeness Centrality  
 189 properties (Table 2).

Table 2. The summary of the significant results in Average Path Length (APL) and Closeness Centrality (CC) in *e4* carriers relative to non-carriers and their interpretation in the context.

Network	APL	CC	Affected Brain Region	Interpretation
Sensorimotor	↓	↓	L postcentral gyrus	The loss of the central role of the

---

Visual	↓	↓	L & R lateral occipital cortex (inferior division)	region but higher integration facilitated by shorter paths within the networks
Default Mode	↑ / ↓	↑ / ↓	L / R lateral occipital cortex (superior division)	Reconfiguration of the roles of specific regions of the network
Saliency	↑	↓	L rostral prefrontal cortex	The loss of the central role of the region and higher segregation facilitated by longer paths within the network
Language	↑	↑	L posterior superior temporal gyrus	The increase of the central role of the region but higher segregation facilitated by longer paths within the network

---

190

191 Average Path Length and Closeness Centrality decreased in *APOEε4* carriers in the left  
192 postcentral gyrus in the sensorimotor network (-55, -12, 29;  $T = -5.64$ ,  $p\text{-FDR} < 0.0001$ ; Fig 2A)  
193 and bilaterally in the inferior division of the lateral occipital cortex in the visual network (-37, -79, 10;  
194 38, -72, 13;  $T = -5.23$ ,  $p\text{-FDR} < 0.0001$ ; Fig 2B). There were no significant differences in the  
195 sensorimotor network globally; however, Degree Centrality, Cost, and Global Efficiency showed a  
196 trend when using an uncorrected p-value ( $T = 2.02$ ,  $p\text{-unc} = 0.0451$ ). A similar trend was observed  
197 in Cost and Global Efficiency in the visual network ( $T = 2.02$ ,  $p\text{-unc} = 0.0451$ ).

198 The opposite pattern was found in the language network, where Average Path Length and  
199 Closeness Centrality increased in the left posterior superior temporal gyrus in *e4* carriers (-57, -47,  
200 15;  $T = 2.71$ ,  $p\text{-FDR} = 0.0316$ ; Fig 2C).

201 The DMN and saliency network showed interesting patterns of differences in graph-theoretical  
202 properties. Firstly, a mixed directionality was observed in the DMN. While Average Path Length  
203 and Closeness Centrality decreased in *APOEε4* carriers in the right superior division of the lateral  
204 occipital cortex (47, -67, 33;  $T = -2.81$ ,  $p\text{-FDR} = 0.0117$ ; Fig 2D), they increased in the left superior  
205 division of the lateral occipital cortex (-39, -77, 33;  $T = 4.74$ ,  $p\text{-FDR} < 0.0001$ ; Fig 2C). The DMN  
206 did not show any global differences on any of the properties; however, an uncorrected trend was  
207 observed in Cost and Global Efficiency ( $T = 2.02$ ,  $p\text{-unc} = 0.0451$ ). There was a simultaneous

208 increase in Average Path Length (-32, 45, 27;  $T = 2.98$ ,  $p\text{-FDR} = 0.0261$ ; Fig 2E) and a decrease  
209 in Closeness Centrality in the left rostral prefrontal cortex in the salience network (-32, 45, 27;  $T = -$   
210  $2.78$ ,  $p\text{-FDR} = 0.0459$ ; Fig 2D). Similarly, no global differences in networks were observed; yet,  
211 almost all graph theoretical properties showed trends when using the uncorrected values, including  
212 Global Efficiency ( $T = 2.17$ ,  $p\text{-unc} = 0.0322$ ), Betweenness Centrality ( $T = 2.02$ ,  $p\text{-unc} = 0.0455$ ),  
213 Closeness Centrality ( $T = 2.03$ ,  $p\text{-unc} = 0.0446$ ), Cost ( $T = 1.99$ ,  $p\text{-unc} = 0.0484$ ), Average Path  
214 Length ( $T = 2.01$ ,  $p\text{-unc} = 0.0461$ ), and Degree Centrality ( $T = 2.01$ ,  $p\text{-unc} = 0.0464$ ). Similar global  
215 trends were observed across graph theory properties in the remaining networks; yet, no results  
216 reached the level of significance when controlling for multiple comparisons.

217 When comparing the results to the results derived using z-scores as a thresholding method with a  
218 correspondingly set threshold level, we observed full or partial consistency in the sensorimotor,  
219 visual, language, and salience networks, which highlights the internal validity of the findings from  
220 these networks. Our findings demonstrate the sensitivity to different brain parcellation methods.  
221 The detailed results of the replications by using different thresholding methods and different brain  
222 parcellation methods derived from the ICA and Power's atlas are summarised in Supplementary  
223 Materials 1.

#### 224 4. Discussion

225 In this study, we investigated the graph-theoretical properties of the resting-state networks in  
226 young adults with *APOEε4* allele. The systematic literature review of brain structure and function in  
227 young *APOEε4* carriers revealed no previous studies have utilised graph theory to study networks  
228 in this demographic<sup>23</sup>; hence, to the best of our knowledge, this is the first study to explore the  
229 properties of multiple resting-state networks of *APOEε4* carriers in young adulthood. We found  
230 significant differences in functional connectivity in the DMN, salience, language, sensorimotor, and  
231 visual networks. Interpreting whether differences in graph-theoretical properties are either  
232 beneficial or detrimental is challenging due to the inherent interdependence among network  
233 characteristics, regional roles, and broader contextual factors. To comprehensively assess the  
234 significance of observed changes, those need to be carefully considered and are discussed below.

##### 235 4.1. The sensorimotor and visual networks

236 A change in Average Path Length implies the average distance between pairs of nodes in the  
237 networks has shortened or prolonged. A simultaneous change in Closeness Centrality of a specific  
238 region indicates a shift in its role within the network and is expected due to the mathematical  
239 relationship of these properties. When there is a simultaneous decrease in these properties, the  
240 region is losing its centrality in terms of efficient communication with the broader network, but it is  
241 also becoming more locally interconnected. In other words, the information exchange between the  
242 nodes in the network is facilitated by shorter paths, contributing to a more tightly integrated and  
243 responsive network.



244 This pattern was observed in the left postcentral gyrus in the sensorimotor network and bilaterally  
245 in the inferior division of the lateral occipital cortex in the visual network. Speculatively, this could  
246 imply that these regions, while less influential in terms of global network dynamics, are fostering  
247 more efficient and direct communication within their surroundings. A decrease in Path Length was  
248 previously observed in a whole-brain network in AD<sup>32</sup>. This could be interpreted as the disruption of  
249 the ‘small-world behaviour’ which was also observed in other studies in AD<sup>33</sup> and in cognitively  
250 healthy adults with AD-related pathology<sup>34</sup>, albeit by using different mechanisms. In contrast with  
251 our study, Sanz-Arigita and colleagues explored whole-brain connectivity in symptomatic AD. The  
252 analysis of the whole brain did not yield any significant differences between *APOEε4* carriers and  
253 non-carriers in our study.

254 Rewiring of the sensorimotor network, which is involved in the integration of sensory information  
255 with motor commands, has been observed in MCI and AD<sup>35</sup> and seems to be modulated by the  
256 *APOE* genotype<sup>36</sup>. Similar findings were reported in visual networks in task-based studies in both  
257 MCI and AD<sup>37</sup>, indicating its association with functions such as spatial localisation, face recognition,  
258 or motor perception that are also progressively disturbed in AD. However, the evidence from  
259 cognitively healthy individuals is still limited.

#### 260 4.2. The DMN, salience, and language networks

261 Both the DMN and the salience network showed a more complex pattern of mixed directionality.  
262 While the Average Path Length and the Closeness Centrality decreased in the right superior  
263 division of the lateral occipital cortex, they increased in the left superior division of the lateral  
264 occipital cortex, which might suggest that the DMN is reconfiguring the communication patterns  
265 and roles of these specific regions. The regions of the parieto-occipital cortex have been previously  
266 linked with early AD pathology such as tau accumulation<sup>38</sup>. The authors proposed the relationship  
267 between the posterior DMN connectivity and tau burden. The underlying mechanisms are still not  
268 clear; however, the disturbances in functional connectivity in the DMN, specifically its posterior  
269 regions, have been consistently reported and studied extensively in MCI and AD (reviewed<sup>39</sup>) and  
270 healthy middle-aged adults with genetic risk factors, mainly the *APOEε4* allele (reviewed<sup>6</sup>).

271 There was an increase in Average Path Length and a decrease in Closeness Centrality in the left  
272 rostral prefrontal cortex in the salience network. Unlike the pattern seen in the sensorimotor and  
273 visual networks, this opposing directionality points to a decrease in network efficiency. The left  
274 rostral prefrontal cortex may be becoming less central in terms of efficient communication with the  
275 broader network and the typical distance required to travel between the regions connecting the left  
276 rostral prefrontal cortex is increasing. This region has been previously linked with network  
277 efficiency mediated by education in elderly individuals with a high proportion of *APOEε4* carriers<sup>40</sup>.  
278 Moreover, broader areas of the prefrontal cortex show consistent disturbances in brain function  
279 and structure in middle-aged *APOEε4* carriers (reviewed<sup>5,41</sup>). Both DMN and salience networks

280 play crucial roles in multiple cognitive processes; therefore, differences in topology in their  
281 functional connectome may signify the alterations in fundamental neural processes that could  
282 contribute to susceptibility to neurodegenerative diseases later in life.

283 A simultaneous increase in Average Path Length and Closeness Centrality that was observed in  
284 the language network of *APOEε4* carriers might suggest a consolidation of the network's structure.  
285 The left posterior superior temporal gyrus seems to be establishing longer paths to reach other  
286 nodes in the language network, indicating greater centrality in facilitating information exchange  
287 across the network. However, this increase in centrality may come at the expense of the local  
288 interconnectedness, potentially leading to a more segregated network structure with fewer direct  
289 connections between directly neighbouring nodes. Segregation of functional networks is a common  
290 phenomenon in AD that has been associated with cognitive performance<sup>42</sup> and resilience<sup>43</sup>, or tau  
291 pathology accumulation<sup>44</sup>.

#### 292 4.3. The limitations and future directions

293 To account for the limited number of brain regions in the Oxford-Harvard atlas, we explored the  
294 networks derived from the Power's atlas and the ICA. While our study demonstrated robustness  
295 across various graph-theory thresholding methods, the findings were sensitive to different  
296 parcellation methods. The choice of brain parcellation can significantly influence outcomes, as  
297 seen in the ageing population<sup>45,46</sup>, possibly due to the brain atlas concordance problem<sup>47</sup> and might  
298 contribute to the observed heterogeneity in functional neuroimaging findings across young  
299 *APOEε4* carriers<sup>23</sup>. Currently lacking a standardised parcellation atlas in neurological and  
300 psychiatric research, future studies should carefully consider their choice, enhancing the  
301 interpretability, generalisability, and clinical applicability of neuroimaging findings. This  
302 consideration may also shed light on the mixed directionality of connectivity differences observed  
303 in young *APOEε4* carriers.

304 While functional connectivity has already contributed substantially to the research of AD, the focus  
305 has predominantly been on symptomatic populations and at-risk middle-aged individuals. Detecting  
306 changes in various networks, such as the DMN, years before the occurrence of clinical symptoms,  
307 and correlating the connectivity measures with cognitive improvement post-treatment<sup>48</sup> indicates  
308 the potential of functional connectivity in pre-symptomatic research. However, introducing more  
309 sophisticated computational approaches, including mathematical and machine learning methods  
310 sensitive to subtle brain changes, can significantly enhance efforts to map vulnerability, even in  
311 early adulthood<sup>16</sup>. This can also increase our understanding of the underlying mechanisms of brain  
312 changes discussed thoroughly in our previous work<sup>49</sup>. By leveraging longitudinal and multimodal  
313 setups, researchers can establish trajectories of brain alterations associated with major AD risk  
314 factors, such as the *APOEε4* allele, and their impact on other brain and cognitive changes  
315 throughout the lifespan.

316 Variations in genetic markers, such as the *APOEε4* allele, may differently impact brain connectivity  
317 depending on ethnic background<sup>14</sup>. Therefore, it is crucial that studies properly account for and  
318 report ethnicity to ensure accurate interpretations of neuroimaging data. Our study adds to the  
319 limited body of evidence that *APOEε4* impacts the brain structure and function in young Chinese  
320 Han adults. Recognising these ethnic-specific factors can aid in generalising conclusions about  
321 brain health and disease susceptibility across different populations and should be of focus in future  
322 studies.

323 Investigating risk and resilience factors associated with AD throughout the lifespan is essential for  
324 biomarker development, early detection of disease, and uncovering novel targets for therapeutic  
325 intervention. However, early adulthood remains a significantly underexplored period. Yet, the  
326 findings may provide the necessary context for how early brain vulnerabilities occur, what mitigates  
327 them, and what other factors have a protective effect. For example, exploring the effect of the *ε2*  
328 allele, which is associated with a lower risk of AD-related neurodegeneration, might uncover new  
329 targets for research on promoting life-long health<sup>50</sup>. The present study lacked the statistical power  
330 to delve into the effect of *ε2* comprehensively, emphasising the need for future research to address  
331 this gap. Understanding both similarities and differences in the mechanisms via which *ε4* and *ε2*  
332 alleles affect the brain structure and function is imperative for developing strategies for AD  
333 prevention and therapeutic intervention.

## 334 5. Conclusions

335 Using graph theoretical analysis of resting-state fMRI, our study showed that in young cognitively  
336 healthy adults, Closeness Centrality and Average Path Length were consistently affected in the  
337 DMN, salience, sensorimotor and visual networks, in the brain areas that have been previously  
338 linked with structural, functional, or pathological changes in AD. Moreover, this study also  
339 underscores the critical role of the methodological choices, particularly in the selection of a brain  
340 parcellation method and the subsequent need for the detailed reporting of the methodological  
341 choices.

## 342 6. Data availability

343 The anonymised data from the present study are available from the corresponding author on  
344 reasonable request.

345

- 346 1. Strittmatter, W. J. *et al.* Apolipoprotein E: High-avidity binding to  $\beta$ -amyloid and increased  
347 frequency of type 4 allele in late-onset familial Alzheimer disease. *Proc. Natl. Acad. Sci. U.*  
348 *S. A.* **90**, 1977–1981 (1993).
- 349 2. Hauser, P. S., Narayanaswami, V. & Ryan, R. O. Apolipoprotein E: From lipid transport to  
350 neurobiology. *Prog. Lipid Res.* **50**, 62–74 (2011).
- 351 3. Wisniewski, T. & Drummond, E. APOE-amyloid interaction: Therapeutic targets. *Neurobiol.*  
352 *Dis.* **138**, (2020).
- 353 4. Raulin, A. C. *et al.* ApoE in Alzheimer's disease: pathophysiology and therapeutic strategies.  
354 *Mol. Neurodegener.* **17**, 1–26 (2022).
- 355 5. Habib, M. *et al.* Functional neuroimaging findings in healthy middle-aged adults at risk of  
356 Alzheimer's disease. *Ageing Res. Rev.* **36**, 88–104 (2017).
- 357 6. Kucikova, L. *et al.* Resting-state brain connectivity in healthy young and middle-aged adults  
358 at risk of progressive Alzheimer's disease. *Neurosci. Biobehav. Rev.* **129**, 142–153 (2021).
- 359 7. Hodgetts, C. J. *et al.* Increased posterior default mode network activity and structural  
360 connectivity in young adult APOE- $\epsilon$ 4 carriers: a multimodal imaging investigation. *Neurobiol.*  
361 *Aging* **73**, 82–91 (2019).
- 362 8. Su, Y. Y. *et al.* APOE polymorphism affects brain default mode network in healthy young  
363 adults: A STROBE article. *Med. (United States)* **94**, (2015).
- 364 9. Shen, J. *et al.* Modulation of APOE and SORL1 genes on hippocampal functional  
365 connectivity in healthy young adults. *Brain Struct. Funct.* **222**, 2877–2889 (2017).
- 366 10. Kucikova, L. *et al.* Genetic risk factors of Alzheimer's Disease disrupt resting-state functional  
367 connectivity in cognitively intact young individuals. *J. Neurol.* **270**, 4949–4958 (2023).
- 368 11. Su, Y. Y. *et al.* Lower functional connectivity of default mode network in cognitively normal  
369 young adults with mutation of APP, presenilins and APOE  $\epsilon$ 4. *Brain Imaging Behav.* **11**,  
370 818–828 (2017).
- 371 12. Zhang, N. *et al.* APOE and KIBRA Interactions on Brain Functional Connectivity in Healthy  
372 Young Adults. *Cereb. Cortex* **27**, 4797–4805 (2017).
- 373 13. Dowell, N. G. *et al.* Structural and resting-state MRI detects regional brain differences in  
374 young and mid-age healthy APOE-e4 carriers compared with non-APOE-e4 carriers. *NMR*  
375 *Biomed.* **29**, 614–624 (2016).
- 376 14. Turney, I. C. *et al.* APOE  $\epsilon$ 4 and resting-state functional connectivity in racially/ethnically  
377 diverse older adults. *Alzheimer's Dement. Diagnosis, Assess. Dis. Monit.* **12**, 1–8 (2020).

- 378 15. Su, Y. Y. *et al.* A 32-Month Follow-Up Study of the Effect of APOE  $\epsilon$ 4 on the Whole Brain  
379 Connection in Young Healthy Individuals. *Neuroscience* **551**, 316–322 (2024).
- 380 16. Huang, W. *et al.* Genetic risks of Alzheimer's by APOE and MAPT on cortical morphology in  
381 young healthy adults. *Brain Commun.* **5**, 1–13 (2023).
- 382 17. Matura, S. *et al.* Differential effects of the ApoE4 genotype on brain structure and function.  
383 *Neuroimage* **89**, 81–91 (2014).
- 384 18. Farahani, F. V., Karwowski, W. & Lighthall, N. R. Application of graph theory for identifying  
385 connectivity patterns in human brain networks: A systematic review. *Front. Neurosci.* **13**, 1–  
386 27 (2019).
- 387 19. Liu, Z. *et al.* Altered topological patterns of brain networks in mild cognitive impairment and  
388 Alzheimer's disease: A resting-state fMRI study. *Psychiatry Res. - Neuroimaging* **202**, 118–  
389 125 (2012).
- 390 20. Deng, S., Sun, L., Chen, W., Liu, X. & Chen, S. Effect of APOE $\epsilon$ 4 on Functional Brain  
391 Network in Patients with Subjective Cognitive Decline: A Resting State Functional MRI  
392 Study. *Int. J. Gen. Med.* **14**, 9761–9771 (2021).
- 393 21. Hojjati, S. H., Ebrahimzadeh, A., Khazaei, A. & Babajani-Feremi, A. Predicting conversion  
394 from MCI to AD using resting-state fMRI, graph theoretical approach and SVM. *J. Neurosci.*  
395 *Methods* **282**, 69–80 (2017).
- 396 22. Wink, A. M. *et al.* Functional brain network centrality is related to APOE genotype in  
397 cognitively normal elderly. *Brain Behav.* **8**, 1–13 (2018).
- 398 23. Kucikova, L. *et al.* The effects of APOE $\epsilon$ 4 allele on cerebral structure , function , and related  
399 interactions with cognition in young adults. *Ageing Res. Rev.* **101**, 102510 (2024).
- 400 24. Ritchie, C. W., Wells, K. & Ritchie, K. The PREVENT research programme-A novel research  
401 programme to identify and manage midlife risk for dementia: The conceptual framework. *Int.*  
402 *Rev. Psychiatry* **25**, 748–754 (2013).
- 403 25. Desikan, R. S. *et al.* An automated labeling system for subdividing the human cerebral  
404 cortex on MRI scans into gyral based regions of interest. *Neuroimage* **31**, 968–980 (2006).
- 405 26. Goldstein, J. M. *et al.* Hypothalamic Abnormalities in Schizophrenia: Sex Effects and  
406 Genetic Vulnerability. *Biol. Psychiatry* **61**, 935–945 (2007).
- 407 27. Makris, N. *et al.* Decreased volume of left and total anterior insular lobule in schizophrenia.  
408 *Schizophr. Res.* **83**, 155–171 (2006).
- 409 28. Power, J. D. *et al.* Functional Network Organization of the Human Brain. *Neuron* **72**, 665–

- 410 678 (2011).
- 411 29. Adamovich, T., Zakharov, I., Tabueva, A. & Malykh, S. The thresholding problem and  
412 variability in the EEG graph network parameters. *Sci. Rep.* **12**, 1–18 (2022).
- 413 30. Bullmore, E. & Sporns, O. Complex brain networks: Graph theoretical analysis of structural  
414 and functional systems. *Nat. Rev. Neurosci.* **10**, 186–198 (2009).
- 415 31. Sporns, O. Graph Theory Methods for the Analysis of Neural Connectivity Patterns.  
416 *Neurosci. Databases* 171–185 (2003) doi:10.1007/978-1-4615-1079-6\_12.
- 417 32. Sanz-Arigita, E. J. *et al.* Loss of ‘Small-World’ Networks in Alzheimer’s Disease: Graph  
418 Analysis of fMRI Resting-State Functional Connectivity. *PLoS One* **5**, (2010).
- 419 33. Supekar, K., Menon, V., Rubin, D., Musen, M. & Greicius, M. D. Network analysis of intrinsic  
420 functional brain connectivity in Alzheimer’s disease. *PLoS Comput. Biol.* **4**, (2008).
- 421 34. Brier, M. R. *et al.* Functional connectivity and graph theory in preclinical Alzheimer’s disease.  
422 *Neurobiol. Aging* **35**, 757–768 (2014).
- 423 35. Agosta, F. *et al.* Sensorimotor network rewiring in mild cognitive impairment and Alzheimer’s  
424 disease. *Hum. Brain Mapp.* **31**, 515–525 (2010).
- 425 36. Wang, J. *et al.* Apolipoprotein E  $\epsilon$ 4 modulates functional brain connectome in Alzheimer’s  
426 disease. *Hum. Brain Mapp.* **36**, 1828–1846 (2015).
- 427 37. Deng, Y., Shi, L., Lei, Y. & Wang, D. Altered topological organization of high-level visual  
428 networks in Alzheimer’s disease and mild cognitive impairment patients. *Neurosci. Lett.* **630**,  
429 147–153 (2016).
- 430 38. Cho, H. *et al.* Excessive tau accumulation in the parieto-occipital cortex characterizes early-  
431 onset Alzheimer’s disease. *Neurobiol. Aging* **53**, 103–111 (2017).
- 432 39. Badhwar, A. P. *et al.* Resting-state network dysfunction in Alzheimer’s disease: A systematic  
433 review and meta-analysis. *Alzheimer’s Dement. Diagnosis, Assess. Dis. Monit.* (2017)  
434 doi:10.1016/j.dadm.2017.03.007.
- 435 40. Franzmeier, N. *et al.* The left frontal cortex supports reserve in aging by enhancing  
436 functional network efficiency Rik Ossenkoppele. *Alzheimer’s Res. Ther.* **10**, 1–12 (2018).
- 437 41. Mak, E. *et al.* Structural neuroimaging in preclinical dementia: From microstructural deficits  
438 and grey matter atrophy to macroscale connectomic changes. *Ageing Res. Rev.* **35**, 250–  
439 264 (2017).
- 440 42. He, Y. *et al.* Functional gradients reveal altered functional segregation in patients with  
441 amnesic mild cognitive impairment and Alzheimer’s disease. *Cereb. Cortex* **33**, 10836–

- 442 10847 (2023).
- 443 43. Ewers, M. *et al.* Segregation of functional networks is associated with cognitive resilience in  
444 Alzheimer's disease. *Brain* **144**, 2176–2185 (2021).
- 445 44. Steward, A. *et al.* Functional network segregation is associated with attenuated tau  
446 spreading in Alzheimer's disease. *Alzheimer's Dement.* **19**, 2034–2046 (2023).
- 447 45. Achard, S. & Bullmore, E. Efficiency and cost of economical brain functional networks. *PLoS*  
448 *Comput. Biol.* **3**, 0174–0183 (2007).
- 449 46. Meunier, D., Achard, S., Morcom, A. & Bullmore, E. Age-related changes in modular  
450 organization of human brain functional networks. *Neuroimage* **44**, 715–723 (2009).
- 451 47. Bohland, J. W., Bokil, H., Allen, C. B. & Mitra, P. P. The brain atlas concordance problem:  
452 Quantitative comparison of anatomical parcellations. *PLoS One* **4**, (2009).
- 453 48. Goveas, J. S. *et al.* Recovery of hippocampal network connectivity correlates with cognitive  
454 improvement in mild Alzheimer's disease patients treated with donepezil assessed by  
455 resting-state fMRI. *J. Magn. Reson. Imaging* **34**, 764–773 (2011).
- 456 49. Kucikova, L., Danso, S. O., Muniz-terrera, G. & Ritchie, C. W. Computational Modeling of  
457 Neural Networks of the Human Brain. 1–20.
- 458 50. Suri, S., Heise, V., Trachtenberg, A. J. & Mackay, C. E. The forgotten APOE allele: A review  
459 of the evidence and suggested mechanisms for the protective effect of APOE e2. *Neurosci.*  
460 *Biobehav. Rev.* **37**, 2878–2886 (2013).
- 461
- 462

463 Acknowledgements:

464 LK conceptualised and designed the study, performed the first-level analysis, drafted the  
465 manuscript, and created figures and tables. LK and AB performed the second-level and graph  
466 theory analyses. JZ collected the data. CMN pre-processed the data. JZ, CRW, and LS set up the  
467 extension of the PREVENT-Dementia study. LS, CMN, GMT, CWR, and JOB provided the  
468 feedback. LS secured the funding, provided the guidance, and oversaw the study. We thank the  
469 members of the Artificial Intelligence and Computational Neuroscience at the University of  
470 Sheffield for their insights, comments, and meaningful discussions.

471 Additional information

472 Competing interest:

473 LK, JZ, AD, CMN, and GMT have no conflicts of interests to disclose. CR is the founder of Scottish  
474 Brain Sciences, and acted as a consultant for Biogen, Eisai, MSD, Actinogen, Roche, and Eli Lilly,  
475 and received payment or honoraria from Roche and Eisai in the past. JOB has acted as a  
476 consultant for TauRx, Novo Nordisk, Biogen, Roche, Lilly and GE Healthcare and received grant or  
477 academic support from Avid/ Lilly, Merck and Alliance Medical. LS acted as a consultant for  
478 Shenzhen MirrorEgo Technology Co. Ltd. This research was supported by the NIHR Sheffield  
479 Biomedical Research Centre (BRC) / NIHR Sheffield Clinical Research Facility (CRF). The views  
480 expressed are those of the authors and not necessarily those of the NHS, the NIHR or the  
481 Department of Health and Social Care (DHSC). LK is the recipient of the Flagship Scholarship of  
482 the Neuroscience Institute, University of Sheffield. AJB was funded by the SURE Scholarship,  
483 University of Sheffield. LS was funded by Alzheimer's Research UK Senior Research  
484 Fellowship (ARUK-SRF2017B-1), the Lewy Body Society (LS002/2019).

485



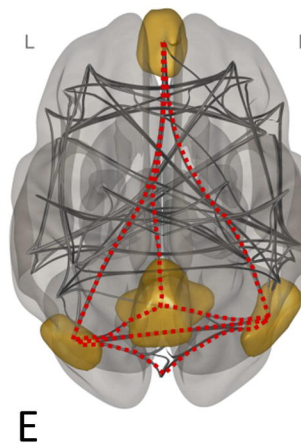
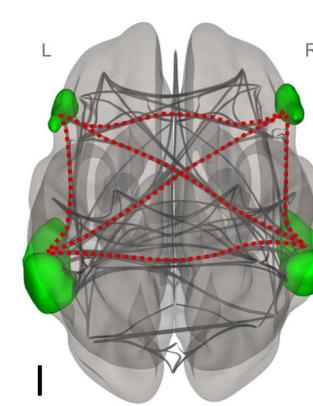
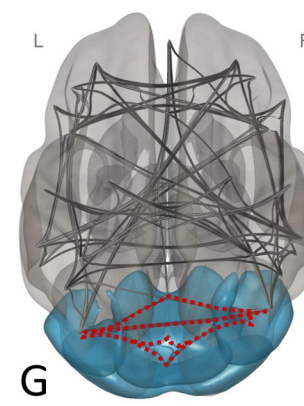
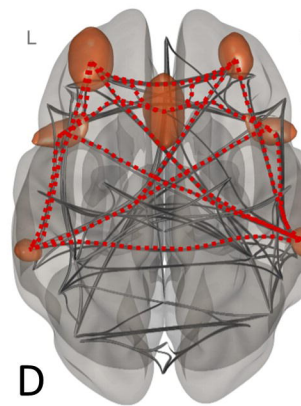
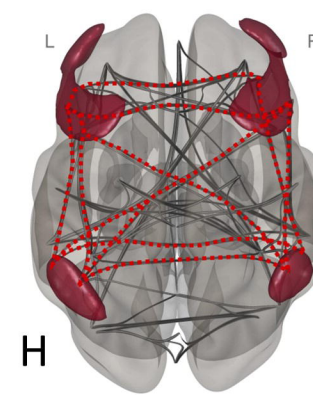
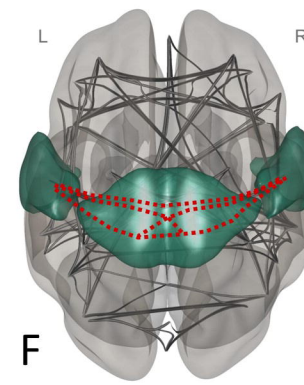
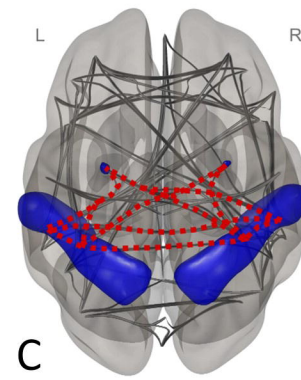
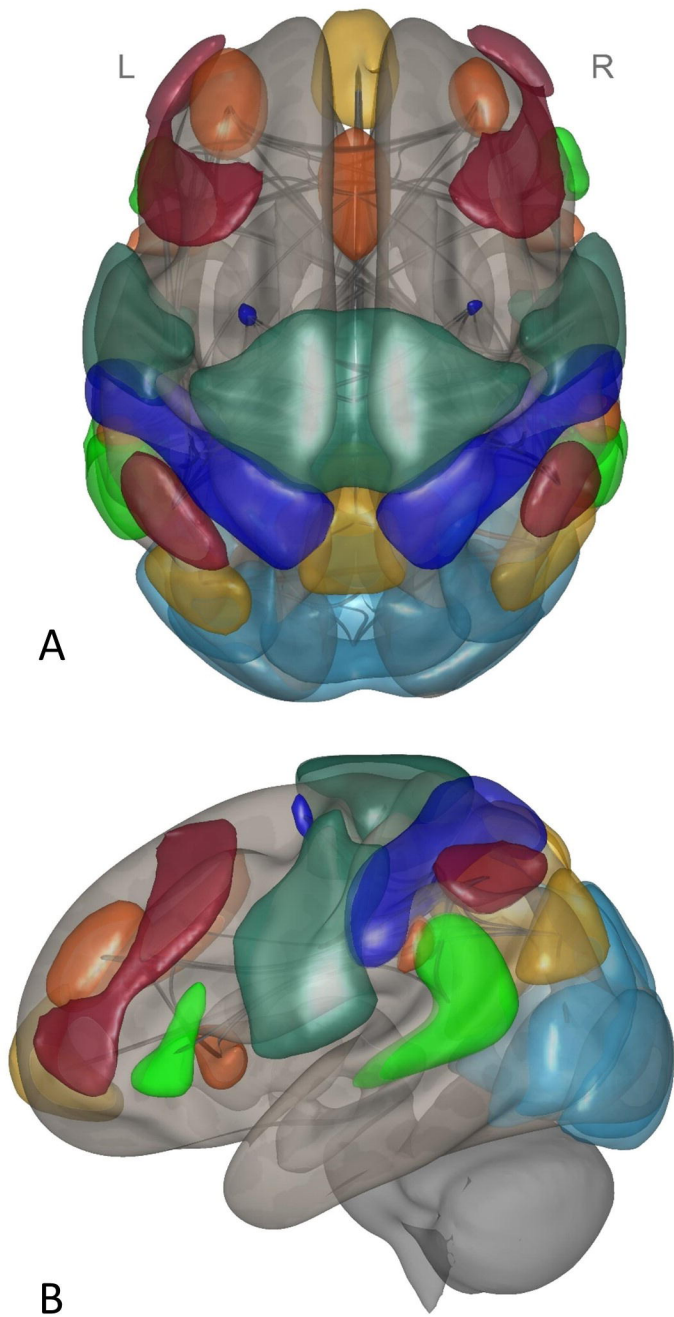
486 Legends:

487 Figure 1. Resting-state networks from the Oxford-Harvard. A) The top-down view of the spatial  
488 maps of all seven networks on the 3D brain. B) The lateral view of the spatial maps of all seven  
489 networks on the 3D brain, C) The graph topology of the Dorsoattentional network, D) The graph  
490 topology of the Frontoparietal network, E) The graph topology of the Default Mode network, F) The  
491 graph topology of the Sensorimotor network, G) The graph topology of the Visual network, H) The  
492 graph topology of the Salience network, I) The graph topology of the Language network.

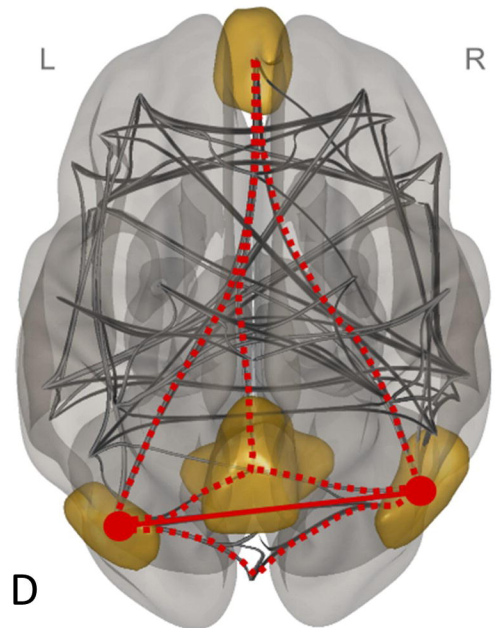
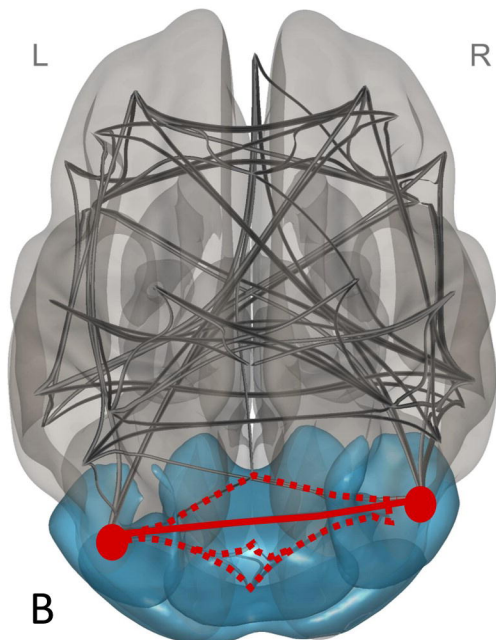
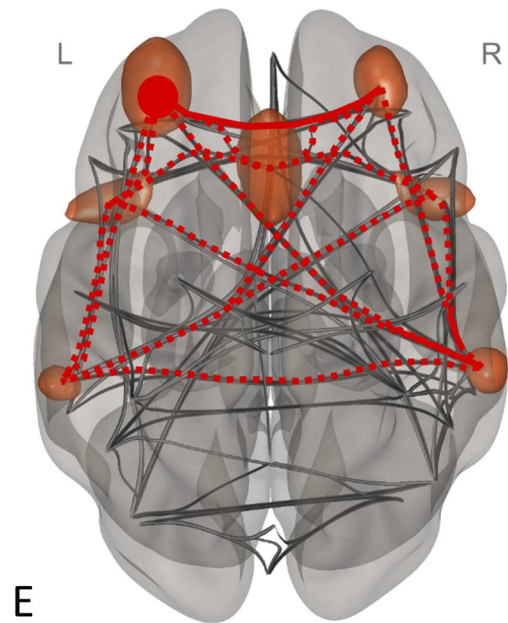
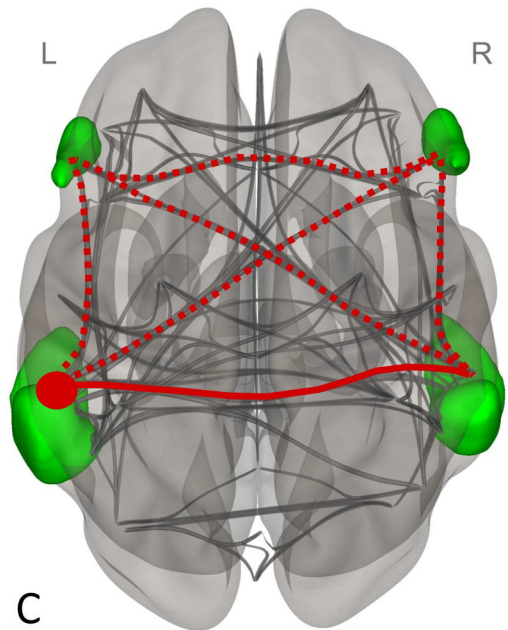
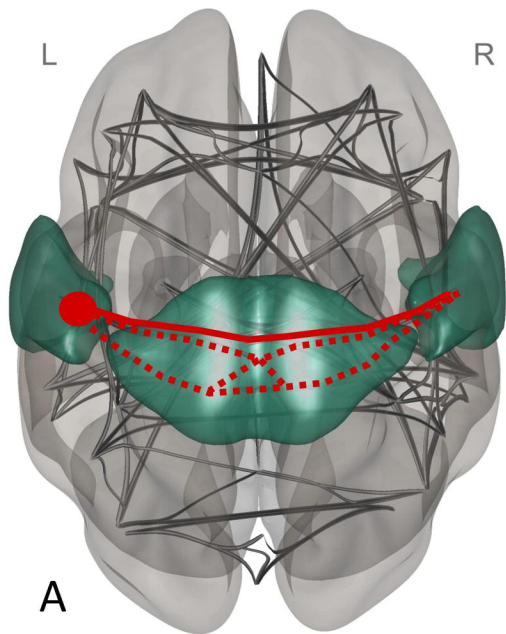
493 Figure 2. The visual representation of the topology of graphs including significant between-group  
494 differences in resting-state networks and respective brain nodes. The topology of the graph is  
495 represented by dotted lines, the significant edges are represented by solid lines, and the significant  
496 hubs are represented by circles. A) Sensorimotor network (left postcentral gyrus). B) Visual  
497 network (bilateral inferior division of the lateral occipital cortex). C) Language network (left posterior  
498 superior temporal gyrus) D) DMN (bilateral superior division of the lateral occipital cortex). E)  
499 Salience network (left rostral prefrontal cortex).

500 Table 1. The summary of the Graph Theory properties studied in the present article.

501 Table 2. The summary of the significant results in Average Path Length (APL) and Closeness  
502 Centrality (CC) in *e4* carriers relative to non-carriers and their interpretation in the context.



— whole-brain graph topology  
- - - network graph topology



- whole-brain graph topology
- ⋯ network graph topology
- significant edge
- significant node